▌Structure Elucidation

Structural Determination of an Unusual Cu^I-Porphyrin-π-Bond in a Hetero-Pacman Cu-Zn-Complex

Michael Marquardt, Beatrice Cula, Vishal Budhija, André Dallmann, and Matthias Schwalbe*[a]

Abstract: The synthesis and characterization of a hetero-dinuclear compound is presented, in which a copper(I) trishistidine type coordination unit is positioned directly above a zinc porphyrin unit. The close distance between the two coordination fragments is secured by a rigid xanthene backbone, and a unique (intramolecular) copper porphyrin-π-bond was determined for the first time in the molecular structure. This structural motif was further analyzed by temperature-dependent NMR studies: In solution at room temperature the coordinative bond fluctuates, while it can be frozen at low temperatures. Preliminary reactivity studies revealed a reduced reactivity of the copper(I) moiety towards dioxygen. The results adumbrate why nature is avoiding metal porphyrin-π-bonds by fixing reactive metal centers in a predetermined distance to each other within multimetallic enzymatic reaction centers.

The enzyme cytochrome c oxidase (CcO) is the biological version of a fuel cell converting dioxygen in a four-electron reduction selectively to two molecules of water with concomitant energy release to drive the translocation of protons across the cell membrane.[1] The cooperative interaction of an iron porphyrin unit (cytochrome a$_3$) and a copper trishistidine unit (Cu$_B$) ensures that no reactive oxygen species, such as hydrogen peroxide, are released during this process.[2] The careful adjustment of the distance between the two metal centers that activate the substrate is crucial for the selectivity of the reaction.

Inspired by this biological blueprint many groups put a lot of effort into designing molecular compounds that resemble the enzymatic reaction center in order to understand its reac-

tion mechanism and, on the other hand, to develop suitable catalysts.[3] The construction of hetero-dinuclear compounds is often tedious and involves multiple reaction steps. Intermolecular systems composed of an iron porphyrin unit and a copper tris-histidine type coordination unit were easier to obtain but showed considerable different reactivity pattern.[3b, c, 4] The fixed distance between the two metal ions in the enzymatic dinuclear reaction center varying between 4.9 and 5.2 Å seems to be very important for the selectivity of the oxygen reduction reaction.[4a, 5] A dangling phenol unit (tyrosine substituent) was also determined to be of crucial importance for proton delivery, that is, proton-coupled electron transfer.[6]

One of the first artificial intramolecular systems to resemble the CcO were developed by Collman et al. and were based on capped or uncapped picket-fence porphyrins.[7] Boitrel and co-workers extended this work to, for example, quinolinoyl picket iron porphyrins that were efficient four-electron reduction catalysts for the reduction of dioxygen to water with or without a copper ion in the distal site.[8] These results put into question if the copper center is essential for the catalytic activity. However, the compound architecture also puts steric congestion around the metal center(s) that might hamper dioxygen uptake and in doing so majorly influences the rate determining step, so that mononuclear, iron-based, O$_2$ activation is facilitated.

Karlin and co-workers designed and synthesized a number of less constrained dinuclear iron copper model complexes in which the proximate copper ion had a clear positive effect on the activation of dioxygen.[9] Intramolecular systems were based on an iron porphyrin tethered to a copper polypyridyl subunit (with or without another axial ligand; see Figure 1 for two examples). Indeed, depending on the ligand architecture, different μ-peroxo intermediates after O$_2$ activation could be determined in their studies.[10] Similarly, Naruta and co-workers reported on the O$_2$ reactivity of dinuclear iron copper complexes, in which a porphyrin unit is either tethered to a tetradentate N4 copper chelate or a tridentate N3 copper chelate with or without a crosslinked histidine-tyrosine mimic (see Figure 1 for one example).[11]

In the latter examples and in CcO the initial activation of dioxygen takes place at a reduced copper center. It is, however, important to note that there are copper(I) compounds that are rather air-stable and show no or considerably decreased reactivity towards O$_2$. The reason for the reduced reactivity was either related to steric crowding or shielded metal frontier orbitals.[12] In addition, Itoh and co-workers investigated dioxy-

[a] M. Marquardt, Dr. B. Cula, V. Budhija, Dr. A. Dallmann, Dr. M. Schwalbe
Institute of Chemistry, Humboldt-Universität zu Berlin
Brook-Taylor-Strasse 2, 12489 Berlin (Germany)
E-mail: matthias.schwalbe@hu-berlin.de

Supporting information and the ORCID identification number(s) for the author(s) of this article can be found under:
https://doi.org/10.1002/chem.202004945.

Chemistry–A European Journal

Communication
doi.org/10.1002/chem.202004945
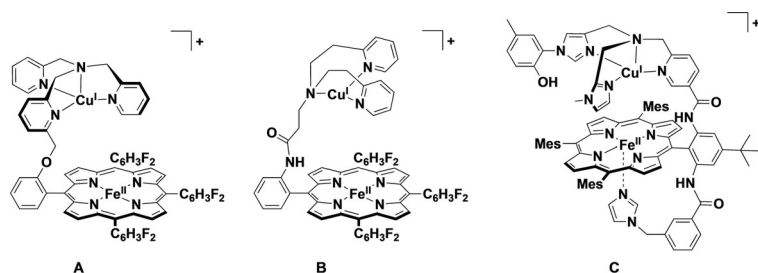
Chemistry
Europe
European Chemical
Societies Publishing

Figure 1. Structure of Fe-Cu model compounds as CcO mimics from Karlin and co-workers (A[9c] and B[9d]) and Naruta and co-workers (C,[11c] Mes = mesityl group).

gen activation with compounds possessing copper(I)-arene π-interactions of η^2-type, including pyridylalkylamine tridentate ligands with appended phenylethylene substituents, and found diminished reactivity.[13]

Thus, different molecular architectures can lead to very different dioxygen activation patterns. There are still only few examples of hetero-dinuclear model compounds known to fully understand the prerequisites necessary for a defined oxygen activation/reduction in this type of catalyst. The used linkers so far are rather flexible, and the influence of a more rigid linker is not well described in literature. Inspired by the work on cofacial diporphyrins, that is, Pacman compounds,[14, 3b] we were interested if a xanthene backbone would lead to a well-defined ligand architecture with the appropriate metal to metal distance to give a new class of CcO mimics and possible oxygen activating molecules.

We here present a hetero-dinuclear compound that shows a unique porphyrin(C=C) π-bond to copper(I), which has never been described before. Surprisingly, the compound shows a strongly retarded reactivity towards dioxygen. The results from this work will not only be important for the design of future hetero-dinuclear compounds but will also be of interest to the biological community in that it provides evidence that nature chose the metal coordination environment in precisely the way to circumvent a Cu^I-porphyrin-π-bond.

The synthesis of title compound $^{Cu}L_{Zn}$ is outlined in the Supporting Information. Briefly, 4-bromo-5-amino-2,7-di-*tert*-butyl-9,9-dimethylxanthene (**3**) is obtained from 4,5-dibromo-2,7-di-*tert*-butyl-9,9-dimethylxanthene in a three-step procedure and further reacted with two equivalents of 2-(chlormethyl)pyridine to give 4-bromo-5-(*N,N*-bis(pyridin-2-yl-methyl)-amino)-2,7-di-*tert*-butyl-9,9-dimethylxanthene (**4**) (Figure 2 and Scheme S1). Latter is combined with 10-(4,4,5,5-tetramethyl-1,3,2-dioxabor-

olyl)-5,15-dimesitylporphyrinato zinc(II) (**5**) in a Pd-catalyzed reaction to give metalloligand L_{Zn} in good yield. Addition of a copper(I) source gives title compound $^{Cu}L_{Zn}$ in basically quantitative yield.

It has to be pointed out that the crucial step in the synthetic procedure is the substitution reaction of **3** to obtain **4**. This reaction has been performed straight-forward with a dibenzofuran backbone instead of a xanthene backbone.[12a] However, the same conditions only led to minor formation of the desired product. Careful optimization of the reaction conditions resulted in formation of **4** in about 70% yield, but only when the concentration of **3**, choice of base (5 equivalents NaH), solvent (THF), and reaction time (three days reflux) were chosen properly. Variation of these parameters caused a strong drop in isolated yield (Table S1). Similarly, several attempts had to be carried out before the optimized Suzuki–Miyaura cross coupling conditions to synthesize L_{Zn} had been obtained (Table S2).

The purity of all new compounds was confirmed by NMR spectroscopy and mass spectrometry (see Supporting Information). Furthermore, it was possible to obtain crystals of L_{Zn} as well as ($^{Cu}L_{Zn}$)PF$_6$ that were suitable for X-ray crystallographic analysis (Table S3); the molecular structures in the solid state are shown in Figure 3.
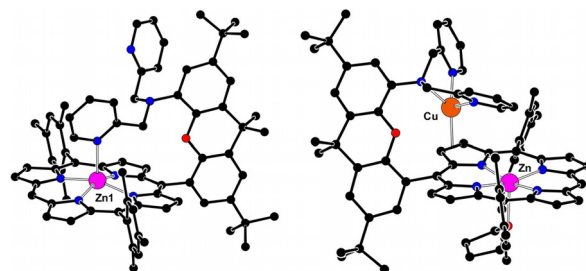

Figure 3. Molecular structures of L_{Zn} (left, only one independent molecule within the unit cell shown) and $^{Cu}L_{Zn}$ (right); hydrogen atoms, counter ions and solvent molecules have been omitted for clarity (except for a THF molecule coordinating as axial ligand to the zinc center in $^{Cu}L_{Zn}$). Further structural information is given in the Supporting Information.

The ^{1}H NMR spectrum of L_{Zn} at room temperature shows a very symmetric signal pattern (Figure 4 and Figure S5), indicating that both pyridyl arms are magnetically equivalent. Surprisingly, the molecular structure shows the coordination of one pyridyl arm to the zinc ion in the porphyrin macrocycle. The
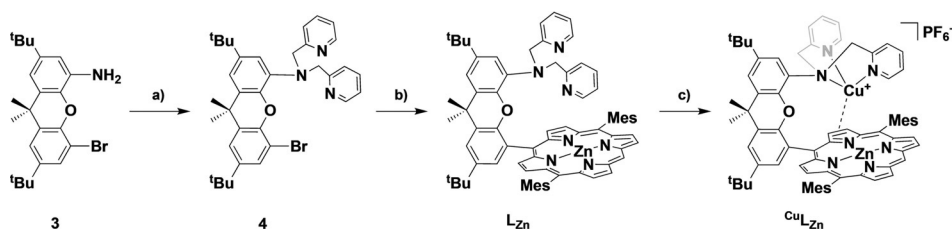

Figure 2. Abbreviated synthesis route towards [$^{Cu}L_{Zn}$]PF$_6$: a) NaH, 2-(chlormethyl)pyridine, THF, reflux, 3 days, 70% yield; b) **5**, Pd(PPh$_3$)$_4$, Cs$_2$CO$_3$, toluene, 90 °C, 24 h, 65% yield; c) [Cu(CH$_3$CN)$_4$]PF$_6$, CH$_3$CN, room temperature, 24 h, >90% yield.

Chemistry–A European Journal

Communication
doi.org/10.1002/chem.202004945

Chemistry Europe
European Chemical
Societies Publishing

bond distances and angles, especially around the square pyramidal coordinated zinc ion, are furthermore not exceptional and reported in the Supporting Information, Figure S23. It seems that only in the solid state the specific coordination of one pyridyl arm occurs while it fluctuates in solution. In order to test this hypothesis, we performed temperature dependent ^{1}H NMR spectroscopy studies on **L$_{Zn}$** in CD$_2$Cl$_2$ solutions (Figures 4 and S15).

At room temperature there are 22 magnetically nonequivalent proton signals. The highest shift is observed for the single proton in *meso*-position of the porphyrin (10.21 ppm) followed by the signals related to the protons in β-position of the porphyrin macrocycle (H^a–H^d; complete numbering Scheme in Figure S5). The signals corresponding to the protons of the pyridyl substituents are markedly shifted to higher field because of the aromatic ring current of the nearby porphyrin macrocycle causing, for example, the signal for H^1 (proton next to the pyridyl nitrogen) to appear at an unusual shift of 4.80 ppm (see also Figures S5–7). Most striking is the strong shift to higher field of the signal for the protons of the methylene groups of the pyridin-2-yl-methyl substituents to 0.73 ppm, while they appear at 4.70 ppm in **4**. Upon cooling, coalescence is observed at about −40°C (Figure S15), and at −80°C a new signal set is appearing that is not as symmetric as has been observed at room temperature. There are two distinguishable sets of signals for the pyridyl substituents now, that can be assigned with the help of 2D NMR experiments, such as exchange spectroscopy (EXSY) (Figures 4 and S16). Thus, the former single signal for H^1 at 4.80 ppm developed into two new signals at 8.07 and 1.33 ppm, that is, a difference of almost 7 ppm! The first signal is in the expected region for a pyridyl proton without intermolecular interactions, while the region for the second signal is very unusual. Furthermore, the single signal for the four methylene protons at 0.73 ppm splits up into four signals at 1.97, 1.44, 0.92, and −1.59 ppm (chemical shifts taken from the EXSY spectrum, Figure S16), which partially overlap with other signals in this region.

Clearly, this behavior is a result of the coordination of one pyridyl arm to the zinc ion, as observed in the solid-state structure. Alternatively, strong π–π-interaction between the porphyrin unit and one pyridyl substituent might be envisioned, but this should not result in such strong shifts. As can be seen in the molecular structure of **L$_{Zn}$**, the (coordinated) bis(pyridinyl-methyl) fragment (Figure S23) causes the mesityl substituents to become magnetically inequivalent explaining the splitting of the former symmetric porphyrin related signal set(s), that is, for the mesityl substituents and β-protons, at low temperature. Such an intramolecular coordinative bond between a pyridyl arm and a zinc porphyrin has rarely been observed,[15] but has similarly been shown for pyridyl iron(porphyrinato) compounds by others.[9b,d]

In case of ^{Cu}**L$_{Zn}$** the molecular structure determined by X-ray crystallography shows an uncommon copper(I)-porphyrin(C=C) π-bond interaction. In fact, we here present, to the best of our knowledge, the first structure in which this motif has been observed. Copper(I)-π-double bond interaction is, however, well known—even intramolecularly.[13b, 16] The overall coordination environment around the copper(I) ion in ^{Cu}**L$_{Zn}$** can be described as distorted tetrahedral (see also Figure S24). The Cu–C distances of 2.107(3) and 2.127(3) Å represent the η^2 coordination mode of one formal double bond of the porphyrin macrocycle occupying one coordination site. Because of the π-backbonding interaction, the C=C bond [C6–C24 = 1.384(4) Å, Figure S24] is elongated by about 0.03 Å compared to the other C=C bonds in the porphyrin macrocycle [average 1.354(4) Å]. Cu–N distances between the two pyridine nitrogen atoms (N$_{Py}$) are surprisingly different with 2.020(2) and 2.114(2) Å, while the bond distance between Cu and tertiary amine nitrogen N$_{am}$ is only slightly longer [2.191(2) Å]. Zinc is coordinated square pyramidal with the four nitrogen atoms of the porphyrin forming the base (average Zn–N$_{por}$ distance is 2.05 Å) and one apical oxygen atom from a THF solvent molecule [Zn-O 2.199(2) Å]. The bond distances and angles within the porphyrin and xanthene unit (reported in the Supporting Information,
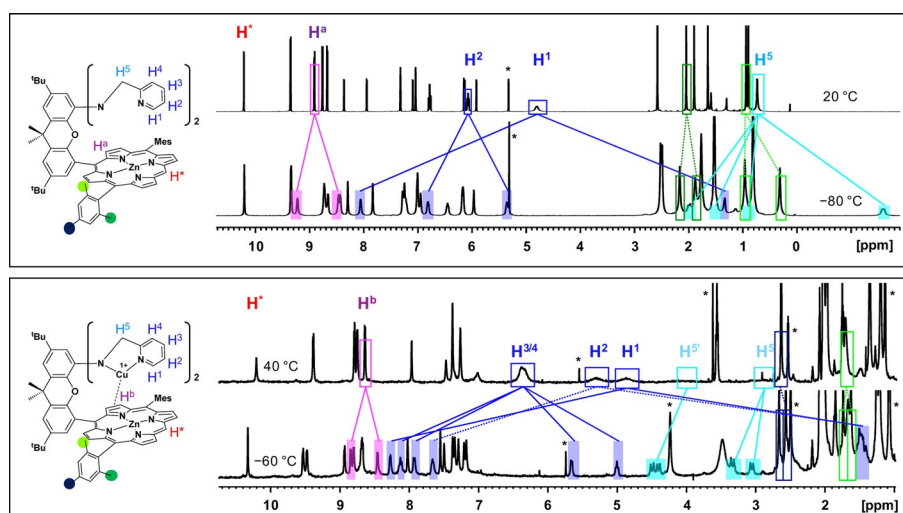

Figure 4. Temperature dependency of ^{1}H NMR spectra (400 MHz) of **L$_{Zn}$** in CD$_2$Cl$_2$ (top) and ^{Cu}**L$_{Zn}$** in [D$_6$]acetone (bottom) with highlighting the strongest splittings/shifts occurring on lowering the temperature (full signal assignment is given in the Supporting Information).

Chemistry–A European Journal

Communication
doi.org/10.1002/chem.202004945

Chemistry Europe
European Chemical
Societies Publishing

Figure S24) are not exceptional to similar published compounds.[17]

^{1}H NMR spectra in several deuterated solvents suffer from line-broadening—especially for the pyridyl related signals (Figures S10, S17–S19). Nevertheless, it is clear that at room temperature always a rather symmetric pattern is observed, which means that the pyridyl arms and mesityl substituents are indistinguishable (see also Figure 4). It can be noted, however, that the pyridyl substituents seem to encounter a stronger ring current effect of the nearby porphyrin, because the related signals show stronger high-field shifts as compared to L_{Zn}. Very likely, fluxional behavior in terms of a quick change of the copper(I) ion from one side of the porphyrin to the other is the reason for this observation, though, at the moment, we cannot rule out possible solvent coordination as competitive reaction; especially in strongly coordinating solvents. Cooling a solution of $^{Cu}L_{Zn}$ in [D_6]acetone causes the disappearance and re-emerging of signals (at different temperatures though, Figure S20) with best resolution noticeable at 213 K (Figure 4). With the help of 2D-NMR experiments (e.g., Figure S22), a complete signal assignment was possible. The pyridyl and mesityl substituents give rise to two sets of signals, which corroborates the results of the crystal structure analysis and the reduced symmetry due to copper coordination to one double bond of the porphyrin macrocycle (Figure S24). There are two broad signals for the four methylene protons at about 4.2 and 2.9 ppm at room temperature that split up into four signals at similar chemical shifts at 213 K (Figure S20). This result indicates that there is not as much of a ring current effect as observed for these signals in L_{Zn}, due to coordination of the copper ion and turning away of the CH_2 groups from the porphyrin plane. The most striking feature to note is again the strong difference of chemical shifts for the proton signals of the pyridyl substituents (Figure 4). For H^1 there are two new signals at 8.3 and 1.4 ppm at 213 K, demonstrating that one pyridyl substituent is located directly above the porphyrin while the other one has almost no through space interaction with latter, as also demonstrated in Figure S24.

In order to get a first idea about the redox properties of title compound $^{Cu}L_{Zn}$, cyclic voltammetry experiments were performed (summarized in Table S4). First, L_{Zn} was investigated in THF solution: Two reduction and two oxidation processes are obvious (Figure S26). The first reduction event at −2.02 V vs. Fc/Fc$^+$ is reversible and based on the porphyrin moiety. All other redox events are irreversible (which does not change by increasing the scan rate). In case of $^{Cu}L_{Zn}$, three reduction and three irreversible oxidation processes are observed (Figure S27). Surprisingly, the position of the first two oxidation events does not change markedly going from L_{Zn} to $^{Cu}L_{Zn}$. The first reduction is quasi-reversible, porphyrin-based, and shifted by about 0.2 V to more positive potential as compared to L_{Zn}. The second reduction process is somehow ill-defined, but partially reversible, while the third reduction at −2.45 V is irreversible. The easier reducibility of the porphyrin macrocycle is very likely the result of the nearby positively charged copper unit that exerts a through-space electron-withdrawing effect. At the moment, we do not have a clear indication of the expected

Cu^I/Cu^{II} couple (reported to be around −0.2 V vs. Fc/Fc$^+$ in CH_2Cl_2 for a mononuclear analogue),[13c] but it might be hidden underneath the oxidation wave at about +0.5 V. Interestingly, there is a wave at −0.5 V arising on the back (cathodic) scan after passing through the first anodic redox event(s) (Figure S27), that might be tentatively assigned to the reduction of an intermediately formed Cu^{II} species. The interpretation of the electrochemical results is supported by comparison to the electrochemical data of reference compound $^{Cu}4$, which is obtained by reaction of 4 with [Cu(CH_3CN)$_4$]PF$_6$ (see Supporting Information). The first irreversible oxidation of $^{Cu}4$ occurs at a peak potential of 0.11 V vs. Fc/Fc$^+$ and is accompanied by a wave at around −0.5 V arising on the back (cathodic) scan (Figure S29), which fits fairly well to the reported values of similar mononuclear copper complexes.

The copper-zinc distance in $^{Cu}L_{Zn}$ is about 4.8 Å, which is a suitable distance to allow for a possible cooperative activation of a substrate molecule, such as dioxygen. Indeed, compound $^{Cu}L_{Zn}$ is air sensitive: Exposing a solution to air or oxygen results in slow transformation to a paramagnetic species, very likely a copper(II) species, as has been proven by ^{1}H NMR (in [D_6]acetone; Figures S31) and electron paramagnetic resonance (EPR) spectroscopy (in CH_2Cl_2; Figure S33). The NMR experiments show slow but steady decrease of the signals for $^{Cu}L_{Zn}$ and the development of unspecific new signals. Unfortunately, broadening does not allow to make any assignments and it can only be concluded that paramagnetic copper(II) species evolve after several hours of reaction time. Interestingly, in a similar experiment compound $^{Cu}4$ reacts with dioxygen and after one hour of reaction time, no signals related to the starting compound can be detected (Figure S32).

To our surprise, recrystallization of an oxidized sample of $^{Cu}L_{Zn}$, provided crystals that were suitable for X-ray crystallographic characterization. The molecular structure of $^{CuCl2}L_{Zn}$ is shown in Figure S25 and demonstrates that the copper ion is now in a +2 oxidation state and a distorted square pyramidal coordination environment with two additional chloride ligands, which very likely stem from CH_2Cl_2 decomposition. Chloride abstraction from halogenated hydrocarbons is a well-known phenomenon in copper(I) chemistry.[18] The five-coordinated copper(II) unit has mononuclear predecessors that were structurally characterized.[19] The τ value[20] of 0.10 is similar to the one reported for the mononuclear counterparts and represents minor distortion from the square-pyramidal geometry. The oxidation of the copper ion is very likely initiated/assisted by dioxygen as no reaction occurs between $^{Cu}L_{Zn}$ and CD_2Cl_2 in [D_6]acetone solution as evidenced by ^{1}H NMR spectroscopy.

Karlin and co-workers investigated the O_2 activation at a copper(I) center coordinated by the tridentate ligand dipicolyl-benzylamin ([Cu^I(^{Bz}L)(CH_3CN)]$^+$) at −80 °C leading to the formation of a dicopper(III)-bis-μ-oxo species.[21] Hence, the reactivity of $^{Cu}L_{Zn}$ (as well as $^{Cu}4$) towards dioxygen was tested further by UV/Vis spectroscopy to get insight into the initial O_2 activation step: Adding dioxygen to a solution of $^{Cu}L_{Zn}$ or $^{Cu}4$ in acetone either at low temperature or at room temperature led to no obvious changes. Similarly, addition of KO$_2$ in acetonitrile or acetone to $^{Cu}L_{Zn}$ only led to very small, but undefined changes.

Chemistry–A European Journal | Communication
doi.org/10.1002/chem.202004945

Chemistry
Europe
European Chemical
Societies Publishing

The intense porphyrin absorptions (see also Figure S30) seem to cover all copper-based changes, which are expected to be less intense.

These results lead to the assumption that the reactivity of the copper(I) complex $^{Cu}L_{Zn}$ is indeed very sluggish, which can be attributed to the nearby xanthene as well as porphyrin macrocycle exerting, on the one hand, a steric congestion/protection and, on the other hand, a through-space interaction. It is important to note, that unreactive copper(I) compounds are infrequently observed in literature and in most cases steric crowding and shielded metal frontier orbitals are the reason for the inactivity towards small molecule, such as dioxygen, activation.[12,13]

In summary, the proximity of the two metal coordination fragments allows for the development of new structural motifs that provides new ideas on why nature chose structural arrangements as it did. In case of $^{Cu}L_{Zn}$ a retarded reactivity towards dioxygen is observed, probably because of a too strong interaction/steric shielding between the porphyrin moiety and the copper N3 side. In the enzyme CcO, the protein environment very likely prevents a Cu^I-porphyrin-π-bond just because of this detrimental effect. Nevertheless, ligand **L** is a very promising platform for the future synthesis and investigation of hetero-dinuclear complexes that may exhibit novel electronic properties and reactivities. The exchange of the zinc ion to iron will give a more suitable metal center to investigate small molecule activation, which is currently investigated in our group.

Acknowledgements

Conflict of interest

The authors declare no conflict of interest.

[1] a) H. Michel, *Biochemistry* **1999**, *38*, 15129–15140; b) E. Kim, E. E. Chufán, K. Kamaraj, K. D. Karlin, *Chem. Rev.* **2004**, *104*, 1077–1133; c) S. Yoshikawa, A. Shimada, *Chem. Rev.* **2015**, *115*, 1936–1989; d) M. Wikström, K. Krab, V. Sharma, *Chem. Rev.* **2018**, *118*, 2469–2490.

[2] a) T. Tsukihara, H. Aoyama, E. Yamashita, T. Tomizaki, H. Yamaguchi, K. Shinzawa-Itoh, R. Nakashima, R. Yaono, S. Yoshikawa, *Science* **1995**, *269*, 1069–1074; b) D. A. Proshlyakov, M. A. Pressler, G. T. Babcock, *Proc. Natl.*

Acad. Sci. USA **1998**, *95*, 8020–8025; c) M. Brunori, A. Giuffrè, P. Sarti, *J. Inorg. Biochem.* **2005**, *99*, 324–336.

[3] a) J. P. Collman, R. Boulatov, C. J. Sunderland, L. Fu, *Chem. Rev.* **2004**, *104*, 561–588; b) W. Zhang, W. Lai, R. Cao, *Chem. Rev.* **2017**, *117*, 3717–3797; c) P. Lang, M. Schwalbe, *Chem. Eur. J.* **2017**, *23*, 17398–17412.

[4] a) E. E. Chufán, S. C. Puiu, K. D. Karlin, *Acc. Chem. Res.* **2007**, *40*, 563–572; b) Z. Halime, M. T. Kieber-Emmons, M. F. Qayyum, S. Mondal, T. Gandhi, S. C. Puiu, E. E. Chufan, A. A. N. Sarjeant, K. O. Hodgson, B. Hedman, E. I. Solomon, K. D. Karlin, *Inorg. Chem.* **2010**, *49*, 3629–3645.

[5] a) S. Yoshikawa, K. Shinzawa-Itoh, R. Nakashima, R. Yaono, E. Yamashita, N. Inoue, M. Yao, M. J. Fei, C. P. Libeu, T. Mizushima, H. Yamaguchi, T. Tomizaki, T. Tsukihara, *Science* **1998**, *280*, 1723–1729; b) W.-G. Han Du, A. W. Götz, L. Noodleman, *Inorg. Chem.* **2019**, *58*, 13933–13944; c) T. Kitagawa, *J. Inorg. Biochem.* **2000**, *82*, 9–18.

[6] a) M. R. A. Blomberg, *Biochemistry* **2016**, *55*, 489–500; b) M. R. A. Blomberg, P. E. M. Siegbahn, *Biochim. Biophys. Acta* **2015**, *1847*, 364–376; c) M. R. A. Blomberg, P. E. M. Siegbahn, *Biochim. Biophy. Acta* **2015**, *1847*, 1173–1180; d) K. Kirchberg, H. Michel, U. Alexiev, *J. Biol. Chem.* **2012**, *287*, 8187–8193.

[7] a) J. P. Collman, *Inorg. Chem.* **1997**, *36*, 5145–5155; b) J. P. Collman, M. Rapta, M. Bröring, L. Raptova, R. Schwenninger, B. Boitrel, L. Fu, M. L'Her, *J. Am. Chem. Soc.* **1999**, *121*, 1387–1388; c) J. P. Collman, N. K. Devaraj, R. A. Decréau, Y. Yang, Y.-L. Yan, W. Ebina, T. A. Eberspacher, C. E. D. Chidsey, *Science* **2007**, *315*, 1565–1568; d) J. P. Collman, R. A. Decréau, *Chem. Commun.* **2008**, 5065–5076.

[8] a) D. Ricard, A. Didier, M. L'Her, B. Boitrel, *ChemBioChem* **2001**, *2*, 144–148; b) A. Didier, M. L'Her, B. Boitrel, *Org. Biomol. Chem.* **2003**, *1*, 1274–1276.

[9] a) E. E. Chufán, B. Mondal, T. Gandhi, E. Kim, N. D. Rubie, P. Moënne-Loccoz, K. D. Karlin, *Inorg. Chem.* **2007**, *46*, 6382–6394; b) M.-A. Kopf, K. D. Karlin, *Inorg. Chem.* **1999**, *38*, 4922–4923; c) R. A. Ghiladi, T. D. Ju, D.-H. Lee, P. Moënne-Loccoz, S. Kaderli, Y.-M. Neuhold, A. D. Zuberbühler, A. S. Woods, R. J. Cotter, K. D. Karlin, *J. Am. Chem. Soc.* **1999**, *121*, 9885–9886; d) E. Kim, J. Shearer, S. Lu, P. Moënne-Loccoz, M. E. Helton, S. Kaderli, A. D. Zuberbühler, K. D. Karlin, *J. Am. Chem. Soc.* **2004**, *126*, 12716–12717.

[10] a) Z. Halime, H. Kotani, Y. Li, S. Fukuzumi, K. D. Karlin, *Proc. Natl. Acad. Sci. USA* **2011**, *108*, 13990–13994; b) S. Chatterjee, K. Sengupta, S. Hematian, K. D. Karlin, A. Dey, *J. Am. Chem. Soc.* **2015**, *137*, 12897–12905.

[11] a) T. Chishiro, Y. Shimazaki, F. Tani, Y. Tachi, Y. Naruta, S. Karasawa, S. Hayami, Y. Maeda, *Angew. Chem. Int. Ed.* **2003**, *42*, 2788–2791; *Angew. Chem.* **2003**, *115*, 2894–2897; b) Y. Naruta, T. Sasaki, F. Tani, Y. Tachi, N. Kawato, N. Nakamura, *J. Inorg. Biochem.* **2001**, *83*, 239–246; c) J.-G. Liu, Y. Naruta, F. Tani, *Angew. Chem. Int. Ed.* **2005**, *44*, 1836–1840; *Angew. Chem.* **2005**, *117*, 1870–1874; d) J.-G. Liu, Y. Naruta, F. Tani, *Chem. Eur. J.* **2007**, *13*, 6365–6378.

[12] a) S. T. Li, B. Braun-Cula, S. Hoof, M. Dürr, I. Ivanović-Burmazović, C. Limberg, *Eur. J. Inorg. Chem.* **2016**, 4017–4027; b) M. Keck, S. Hoof, V. Rawat, A. Vigalok, C. Limberg, *Z. Anorg. Allg. Chem.* **2020**, *646*, 904–908 and references cited therein.

[13] a) T. Osako, Y. Tachi, M. Taki, S. Fukuzumi, S. Itoh, *Inorg. Chem.* **2001**, *40*, 6604–6609; b) T. Osako, Y. Tachi, M. Doe, M. Shiro, K. Ohkubo, S. Fukuzumi, S. Itoh, *Chem. Eur. J.* **2004**, *10*, 237–246; c) T. Osako, Y. Ueno, Y. Tachi, S. Itoh, *Inorg. Chem.* **2003**, *42*, 8087–8097.

[14] a) J. Rosenthal, D. G. Nocera, *Prog. Inorg. Chem.* **2007**, *55*, 483–544; b) J. P. Collman, P. S. Wagenknecht, J. E. Hutchison, *Angew. Chem. Int. Ed. Engl.* **1994**, *33*, 1537–1554; *Angew. Chem.* **1994**, *106*, 1620–1639.

[15] a) A. Hamazawa, T. Yano, T. Nishioka, I. Kinoshita, K. Isobe, S. Yano, L. J. Wright, T. J. Collins, *Chem. Lett.* **2003**, *32*, 20–21; b) S. Venkataramani, U. Jana, M. Dommaschk, F. D. Sönnichsen, F. Tuczek, R. Herges, *Science* **2011**, *331*, 445–448; c) J. Tanihara, K. Ogawa, Y. Kobuke, *J. Photochem. Photobiol. A* **2006**, *178*, 140–149.

[16] a) R. Crescenzi, E. Solari, C. Floriani, A. Chiesi-Villa, C. Rizzoli, *J. Am. Chem. Soc.* **1999**, *121*, 1695–1706; b) Y. Shimazaki, H. Yokoyama, O. Yamauchi, *Angew. Chem. Int. Ed.* **1999**, *38*, 2401–2403; *Angew. Chem.* **1999**, *111*, 2561–2563; c) ref. [13c] and references cited therein.

[17] a) P. Lang, M. Pfrunder, G. Quach, B. Braun-Cula, E. G. Moore, M. Schwalbe, *Chem. Eur. J.* **2019**, *25*, 4509–4519; b) M. Schwalbe, P. Wrzolek, G. Lal, B. Braun, *Eur. J. Inorg. Chem.* **2014**, 4209–4217, and references therein.

[18] a) Z. Tyeklar, R. R. Jacobson, N. Wei, N. N. Murthy, J. Zubieta, K. D. Karlin, *J. Am. Chem. Soc.* **1993**, *115*, 2677–2689; b) R. R. Jacobson, Z. Tyeklár, K. D. Karlin, *Inorg. Chim. Acta* **1991**, *181*, 111–118; c) A. W. Maverick, M. L. Ivie, F. R. Fronczek, *J. Coord. Chem.* **1990**, *21*, 315–322.

[19] a) A. Bhattacharyya, A. Dixit, S. Banerjee, B. Roy, A. Kumar, A. A. Karande, A. R. Chakravarty, *RSC Adv.* **2016**, *6*, 104474–104482; b) K. A. Bussey, A. R. Cavalier, M. E. Mraz, K. D. Oshin, A. Sarjeant, T. Pintauer, *Polyhedron* **2016**, *114*, 256–267.

[20] A. W. Addison, T. N. Rao, *J. Chem. Soc. Dalton Trans.* **1984**, 1349–1356.

[21] H. R. Lucas, L. Li, A. A. Narducci Sarjeant, M. A. Vance, E. I. Solomon, K. D. Karlin, *J. Am. Chem. Soc.* **2009**, *131*, 3230–3245.